

AGREEMENT BETWEEN THE WHITE MATTER CONNECTIVITY BASED ON THE TENSOR-BASED MORPHOMETRY AND THE VOLUMETRIC WHITE MATTER PARCELLATIONS BASED ON DIFFUSION TENSOR IMAGING

*Seung-Goo Kim*¹ *Hyekyoung Lee*^{1,2,3} *Moo K. Chung*^{1,4,5,*} *Jamie L. Hanson*^{5,6}
*Brian B. Avants*⁷ *James C. Gee*⁷ *Richard J. Davidson*^{5,6} *Seth D. Pollak*^{3,6}

¹Department of Brain and Cognitive Sciences, ² Department of Nuclear Medicine,

³ Institute of Radiation Medicine, Medical Research Center, Seoul National University, Korea.

⁴ Department of Biostatistics and Medical Informatics,

⁵ Waisman Laboratory for Brain Imaging and Behavior,

⁶ Department of Psychology, University of Wisconsin, Madison, WI, USA.

⁷ Penn Image Computing and Science Laboratory, Department of Radiology,
University of Pennsylvania, Philadelphia, PA, USA.

ABSTRACT

We are interested in investigating white matter connectivity using a novel computational framework that does not use diffusion tensor imaging but only uses T1-weighted magnetic resonance imaging. The method we have been proposed relies on correlating Jacobian determinants across different voxels based on the tensor-based morphometry framework. In this paper, we show high agreement between the TBM-based network and the DTI-based white matter atlas. As an application, altered white matter connectivity in a clinical population is determined.

Index Terms— structural connectivity, brain network, tensor-based morphometry, white matter atlas

1. INTRODUCTION

We aim to investigate white matter connectivity using a novel computational framework that does not rely on diffusion tensor imaging (DTI) [1]. This new method instead uses T1-weighted MRI and relies on correlating Jacobian determinants (JD), which quantifies local tissue volume based on tensor-based morphometry (TBM) [2].

The idea of correlating local morphological features to construct a structural brain network had been considered earlier [3, 4]. The previous works mainly focused on the cortico-

cortical connectivity using cortical thickness [3], which is defined along the gray matter. Therefore, cortical thickness cannot be used in characterizing the connectivity within the white matter. To overcome the limitation of the previous studies, we have proposed to use the JD in constructing the white matter connectivity [1]. Previously, we demonstrated that it is possible to use T1-weighted MRI in characterizing a population-based white matter connectivity [1].

We will show that there is high agreement between the TBM-based network and the DTI-based white matter atlas for the first time in this paper. As a direct application, we compare the TBM-based networks of children who experienced early maltreatment to the normal controls and determine the regions of abnormal white matter connectivity.

2. METHODS

2.1. Subjects and preprocessing

T1-weighted MRI were collected using a 3T GE SIGNA scanner 32 children who experienced maltreatment in their early stage of life in orphanages in East Europe and China but later adopted to the families in US (post-institutionalized; PI) and age-matched 33 normal controls (NC). Two groups were matched for age. The mean age for PI is 11.19 ± 1.73 years while that of NC is 11.48 ± 1.62 years. There are 13 boys and 19 girls in PI, and 20 boys and 13 girls in NC. A study-specific template construction and non-linear normalization of individual images were done by Advanced Normalization Tools (ANTS) [5].

The correspondence should be sent to M.K.C (mkchung@wisc.edu). This work was supported by National Institutes of Health Research Grants MH61285 and MH68858 to S.D.P., funded by the National Institute of Mental Health and the Childrens Bureau of the Administration on Children, Youth and Families as part of the Child Neglect Research Consortium, as well as National Institute of Mental Health Grant MH84051 to R.J.D. This research was also supported by World Class University program through the Korea Science and Engineering Foundation funded by the Ministry of Education, Science and Technology (R31-10089) to M.K.C.

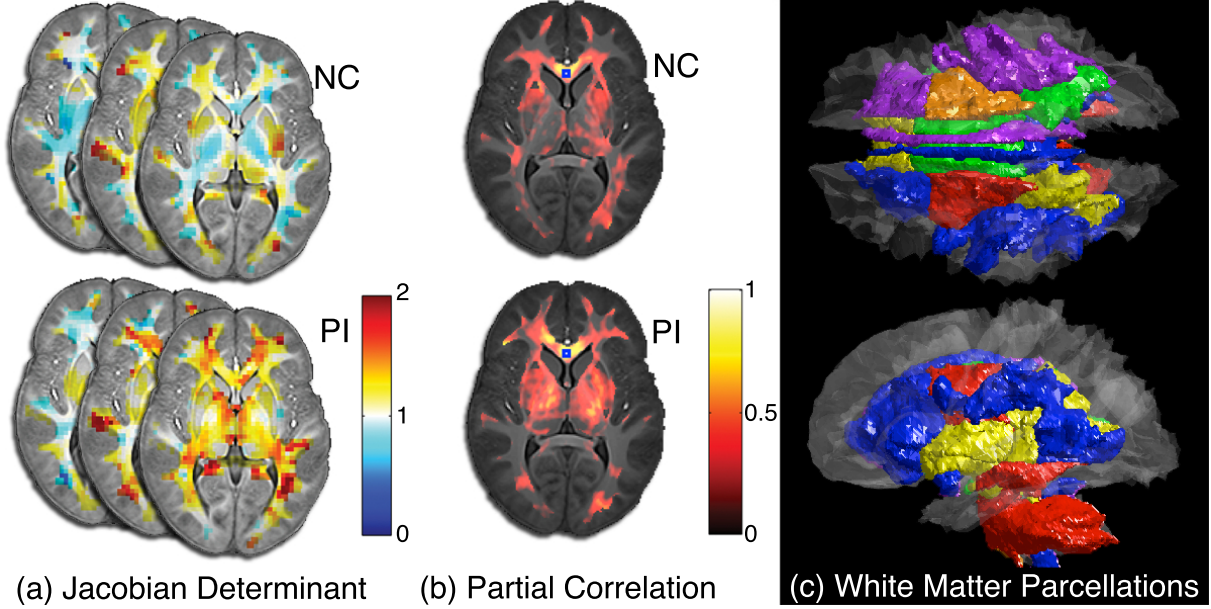


Fig. 1. Illustration of TBM-based connectivity. First JD is computed (a), partial correlation is computed factoring out age and gender (b). Then it is compared to given the white matter parcellations based on DTI (c).

2.2. Partial correlation on Jacobian determinants

Once we obtain the deformation field from the individual MRI to the template, we compute JD. The JD maps were smoothed with a Gaussian kernel with 2mm FWHM. Then we correlate JD across different voxels. The details on constructing JD-based correlation maps is given in [1]. Among the 336363 voxels with white matter density larger than 0.8, 12484 voxels were subsampled at every 3mm as possible network nodes. For nodes i and j , we computed partial correlations $\widehat{\rho}_{ij}$ of JD while factoring out the confounding effect of age and gender. This is done as follows. (1) We start by fitting a general linear model (GLM) of the form as

$$JD = \lambda_0 + \lambda_1 \cdot \text{age} + \lambda_2 \cdot \text{gender} + \text{noise}$$

at each node independently using the least squares method. (2) Compute the residual between the observation and the model fit at each node. (3) Compute the Pearson correlation between the residuals on nodes i and j . This Pearson correlation is the partial correlation. We will only consider positive correlations as conventionally investigated in the many structural brain network studies [6]. This process of constructing TBM-based white matter connectivity is illustrated in Fig. 1

2.3. Connectivity between parcellations

The constructed partial correlation maps were compared against the DTI-based white matter atlas (ICBM-DTI-81) [7]. In the atlas, 50 anatomical subregions in white matter were manually parcellated by radiologists guided by the fractional anisotropy (FA) map and the orientation map based on DTI.

The atlas does not segment all the white matter voxels into partitions, but only labels reliably identifiable voxels that correspond to the major fiber bundles such as corpus callosum, corona radiata and longitudinal fasciculus.

The ICBM-DTI-81 white matter parcellations are given in the MNI-152 template. In order to normalize the white matter parcellations into our study-specific template, we first warped the MNI-152 T1-weighted template into our template, then applied the displacement to the parcellations. Fig. 1 (c) shows the superimposition of the 50 parcellations onto our template space. We assume that, if the white matter connectivity obtained from TBM follows that from DTI, the connectivity within a parcellation will be greater than the connectivity between different parcellations.

The set $\mathcal{C}_k (k = 1, \dots, 48)$ contains a collection of nodes that belongs to the parcellation k . We do not have any nodes in \mathcal{C}_{49} and \mathcal{C}_{50} possibly because the parcellations are too small, thus they are excluded in further analysis. The connectivity matrix \mathbf{X} between the parcellations is given by averaging $\widehat{\rho}_{ij}$ over all possible connections as

$$X_{mn} = \frac{\sum_{i \in \mathcal{C}_m, j \in \mathcal{C}_n, i \neq j} \widehat{\rho}_{ij}}{|\mathcal{C}_m| |\mathcal{C}_n| - \delta_{mn} |\mathcal{C}_m|}, \quad (1)$$

where $|\cdot|$ is the number of elements in a set \cdot and δ_{mn} is 1 ($m = n$) or 0 ($m \neq n$).

The diagonal elements in \mathbf{X} measure connectivity within each parcellation. We call the diagonal term as *within-connectivity* in this paper. On the other hand, the off-diagonal elements measure connectivity between two different parcellations, called as *between-connectivity*. In actual brains, it

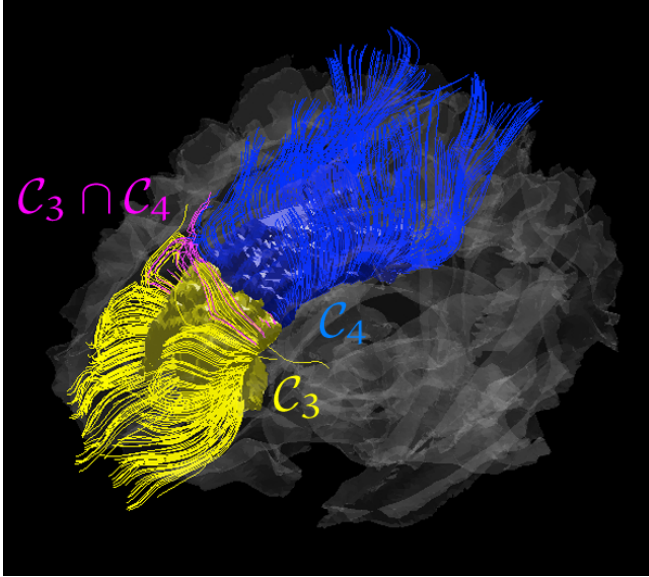


Fig. 2. An example of DTI fiber tracts that pass through the distinct parcellations \mathcal{C}_3 (yellow) and \mathcal{C}_4 (blue) and the tracts that pass through both parcellations $\mathcal{C}_3 \cap \mathcal{C}_4$ (magenta).

is expected that there is no or minimal connectivity between distinct white matter clusters. To illustrate it, an example of white matter tracts constructed from the DTI measurement of a different subject from the current dataset are given in Fig. 2. Note that the overlapping tracts of two parcellations \mathcal{C}_3 (the genu of corpus callosum) and \mathcal{C}_4 (the body of corpus callosum) are only the ones that pass around the boundary between the two parcellations.

Thus, if the TBM-based connectivity map really follows the underlying white matter connectivity, the within-connectivity should be relatively larger than the between-connectivity. As null models with no meaningful connections, 500 random networks were generated where the entries ρ_{ij} are uniformly distributed random variables in $[0,1]$. Then corresponding connectivity matrices are also computed as (1). Connectivity matrices for NC-, PI-networks and one of 500 random networks are shown in Fig. 3.

We tested if the median of within-connectivity is different to that of between-connectivity using the Wilcoxon rank sum test as a non-parametric test. Since we have only one connectivity matrix for a group, we used jackknifing for inferences.

In addition, we tested if the connectivity is different between the PI and the NC for each element. We assumed only diagonal elements are valid to compare pair-wisely, since the off-diagonal elements are supposed to be noise. The p -values were Bonferroni-corrected for multiple comparison corrections.

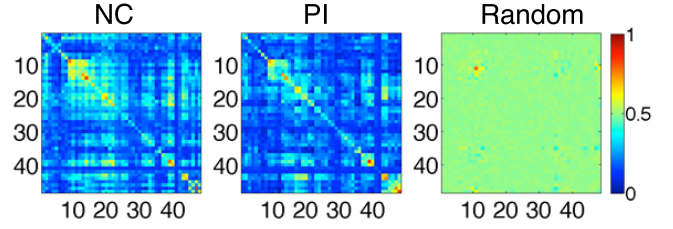


Fig. 3. Estimated connectivity between \mathcal{C}_m and \mathcal{C}_n for NC, PI and one of random network, respectively

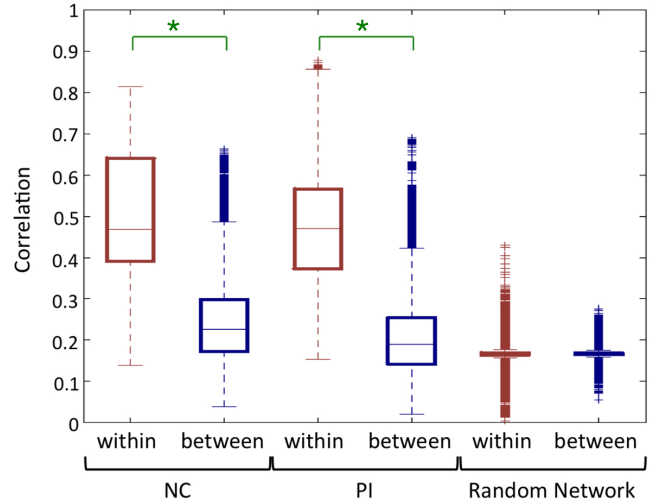


Fig. 4. Wilcoxon rank sum test on connectivity in the NC-, the PI- and random network, respectively. Significant differences between the within-connectivity and the between-connectivity are indicated with asterisks at $\alpha = 0.001$.

3. RESULTS

The median of the within-connectivity is significantly greater than that of the between-connectivity both in the NC- and PI-networks ($p < 0.001$) whereas the difference is not significant in the random networks ($p = 0.37$) (Fig. 4).

For the local inferences, we found significant differences in the within-connectivity between the NC and the PI at Bonferroni corrected $p < 0.01$. The spatial dispositions of significant differences are shown in Fig. 5. We found smaller connectivity at the genu of corpus callosum (GCC) connecting anterior regions of hemispheres, and at the left superior corona radiata (SCR-L) connecting hypothalamic projection to the superior regions of neocortex. We also found greater connectivities at three fiber bundles as well.

4. DISCUSSION AND CONCLUSION

The diagonal elements in the connectivity matrices of the human brains are significantly greater than the off-diagonal ele-

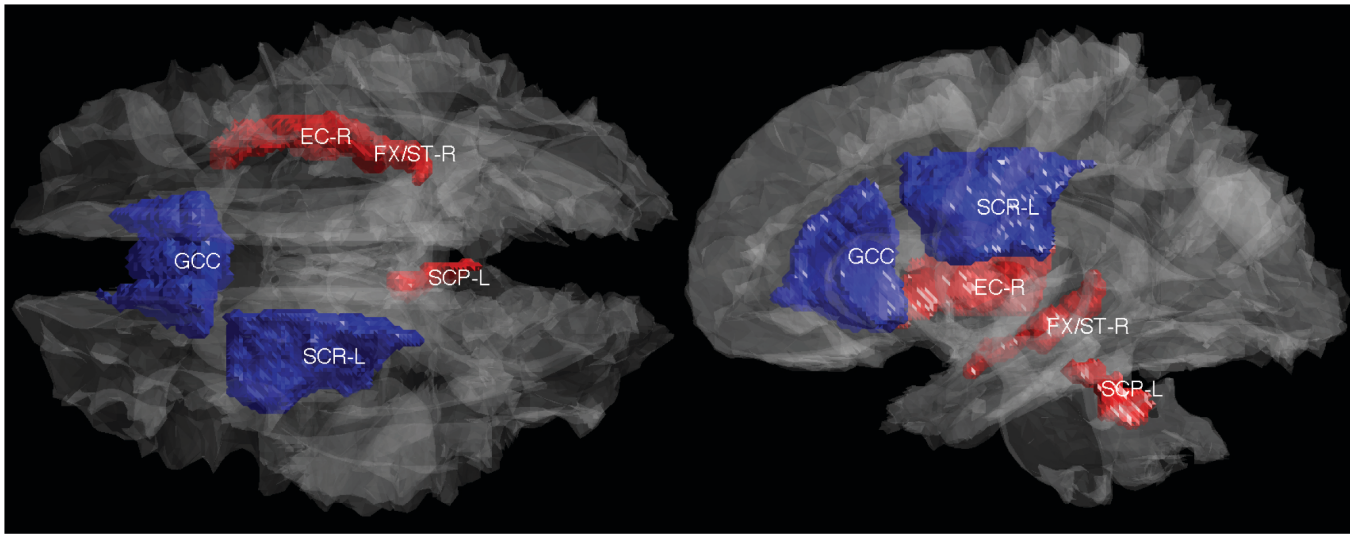


Fig. 5. White matter parcellations that shows group differences in the connectivity between NC and PI. The averaged correlation is greater in the PI than the NC (red) at the right external capsule (EC-R), the right fornix and stria terminalis (FX/ST-R), the left superior cerebellar peduncle (SCP-L). The averaged correlation is smaller in the PI than the NC (blue) at the genu of corpus callosum (GCC) and the left superior corona radiata (SCR-L).

ments unlike that of the random networks. The result suggests that the connectivity map using TBM is in agreement with the existing white matter fiber bundles.

In addition, for some white matter partitions, the within-connectivities were locally different between groups. According to a recent review [8], severe stress during the early developmental stage is found to related to atrophy in some structures including in the corpus callosum. Our result may be related to an altered integrities of white matter connectivity due to early maltreatment.

5. REFERENCES

- [1] S.-G. Kim, M.K. Chung, J.L. Hanson, B.B. Avants, J.C. Gee, R.J. Davidson, and S.D. Pollak, "Structural connectivity via the tensor-based morphometryensor-based morphometry," in *IEEE International Symposium on Biomedical Imaging: From Nano to Macro*, 30 2011-april 2 2011, pp. 808–811.
- [2] M.K. Chung, K.J. Worsley, T. Paus, D.L. Cherif, C. Collins, J. Giedd, J.L. Rapoport, , and A.C. Evans, "A unified statistical approach to deformation-based morphometry," *NeuroImage*, vol. 14, pp. 595–606, 2001.
- [3] J.P. Lerch, K. Worsley, W.P. Shaw, D.K. Greenstein, R.K. Lenroot, J. Giedd, and A.C. Evans, "Mapping anatomical correlations across cerebral cortex (MACACC) using cortical thickness from MRI," *Neuroimage*, vol. 31, no. 3, pp. 993–1003, 2006.
- [4] K.J. Worsley, J.I. Chen, J. Lerch, and A.C. Evans, "Comparing functional connectivity via thresholding correlations and singular value decomposition," *Philosophical Transactions of the Royal Society B: Biological Sciences*, vol. 360, no. 1457, pp. 913, 2005.
- [5] BB Avants, CL Epstein, M. Grossman, and JC Gee, "Symmetric diffeomorphic image registration with cross-correlation: Evaluating automated labeling of elderly and neurodegenerative brain," *Medical image analysis*, vol. 12, no. 1, pp. 26, 2008.
- [6] Y. He, Z. Chen, and A. Evans, "Structural insights into aberrant topological patterns of large-scale cortical networks in alzheimer's disease," *Journal of Neuroscience*, vol. 28, no. 18, pp. 4756, 2008.
- [7] S. Mori, K. Oishi, H. Jiang, L. Jiang, X. Li, K. Akhter, K. Hua, A.V. Faria, A. Mahmood, R. Woods, et al., "Stereotaxic white matter atlas based on diffusion tensor imaging in an ICBM template," *Neuroimage*, vol. 40, no. 2, pp. 570–582, 2008.
- [8] Andrea Parolin Jackowski, Celia de Araujo, Acioly de Lacerda, de Jesus, and Joan Kaufman, "Neurostructural imaging findings in children with post-traumatic stress disorder: Brief review," *Psychiatry and Clinical Neurosciences*, vol. 63, no. 1, pp. 1–8, 2009.